Cancer Cell
Article

Hdac3 Is Essential for the Maintenance of Chromatin Structure and Genome Stability

Srividya Bhaskara,[1] Sarah K. Knutson,[1] Guochun Jiang,[2,3] Mahesh B. Chandrasekharan,[1] Andrew J. Wilson,[4] Siyuan Zheng,[5,6] Ashwini Yenamandra,[7] Kimberly Locke,[8] Jia-ling Yuan,[1] Alyssa R. Bonine-Summers,[1] Christina E. Wells,[1] Jonathan F. Kaiser,[1] M. Kay Washington,[9] Zhongming Zhao,[3,5,6,9] Florence F. Wagner,[10] Zu-Wen Sun,[1,9] Fen Xia,[2] Edward B. Holson,[10] Dineo Khabele,[3,4,9] and Scott W. Hiebert[1,9,*]
[1]Department of Biochemistry, Vanderbilt University, Nashville, TN 37232, USA
[2]Department of Radiation Oncology
[3]Department of Cancer Biology
[4]Division of Gynecologic Oncology, Department of Obstetrics and Gynecology
Vanderbilt University Medical Center, Nashville, TN 37212, USA
[5]Department of Biomedical Informatics
[6]Bioinformatics Resource Center
Vanderbilt University School of Medicine, Nashville, TN 37232, USA
[7]Department of Pathology, Vanderbilt University, Nashville, TN 37232, USA
[8]PathGroup, Nashville, TN 37211, USA
[9]Vanderbilt-Ingram Cancer Center, Vanderbilt University School of Medicine, Nashville, TN 37232, USA
[10]The Broad Institute of MIT and Harvard, 7 Cambridge Center, Cambridge, MA 02142, USA
*Correspondence: scott.hiebert@vanderbilt.edu
DOI 10.1016/j.ccr.2010.10.022

SUMMARY

Hdac3 is essential for efficient DNA replication and DNA damage control. Deletion of *Hdac3* impaired DNA repair and greatly reduced chromatin compaction and heterochromatin content. These defects corresponded to increases in histone H3K9,K14ac; H4K5ac; and H4K12ac in late S phase of the cell cycle, and histone deposition marks were retained in quiescent *Hdac3*-null cells. Liver-specific deletion of *Hdac3* culminated in hepatocellular carcinoma. Whereas *HDAC3* expression was downregulated in only a small number of human liver cancers, the mRNA levels of the HDAC3 cofactor *NCOR1* were reduced in one-third of these cases. siRNA targeting of *NCOR1* and *SMRT* (*NCOR2*) increased H4K5ac and caused DNA damage, indicating that the HDAC3/NCOR/SMRT axis is critical for maintaining chromatin structure and genomic stability.

INTRODUCTION

Histone deacetylases (HDACs) play major roles in modulating chromatin accessibility during transcription, replication, recombination, and repair (Gallinari et al., 2007; Goodarzi et al., 2009), yet the role of individual HDACs in these processes is still unclear. Deacetylation of histones is required for re-establishing chromatin structure on a local basis after transcription of a gene or after the repair of a DNA double-strand break (Tsukamoto et al., 1997). On a global scale, HDACs act during DNA replication when the cellular histone content is doubled, as these newly synthesized histones are acetylated prior to their deposition onto nascent DNA. The residues most commonly associated with this process are H4K5ac and H4K12ac (Sobel et al., 1995; Taddei et al., 1999). These modifications presumably allow histone chaperones to configure the nucleosome correctly before deacetylation stabilizes the nucleosome and/or allows higher-order compaction of the chromatin and the formation of

Significance

Broad-spectrum histone deacetylase inhibitors (HDI) are being used to treat a variety of cancers, and more selective inhibitors are being developed for therapeutic uses. Genetic analysis of individual histone deacetylases (HDACs) is essential to understand the action of these inhibitors and their potential side effects. We show that inactivation of *Hdac3*, a central target of all currently used HDIs, causes genomic instability, and deletion of *Hdac3* in the liver leads to hepatocellular carcinoma. These phenotypes correlate with global increases in the acetylation of specific histone residues, disruptions in chromatin structure, and a loss of heterochromatin. Our results genetically link the HDAC3/NCOR/SMRT axis to the maintenance of critical cell-cycle functions and genomic stability.

heterochromatin (Luger et al., 1997; Luger and Richmond, 1998; Neumann et al., 2009; Verreault et al., 1996).

This process of histone acetylation/deacetylation is required for genomic stability and cell viability, as perturbations in the acetyltransferase or components of this pathway cause genomic instability and result in a failure to recover from genotoxic stress (Clarke et al., 1999; Han et al., 2007; Smith et al., 1998; Yuan et al., 2009). This is a dynamic process that occurs across the entire genome, and the role of HDACs in the re-establishment of chromatin structure after replication is one of the least explored areas of their action. As such, genetic methods have been the most informative approaches to understand the physiological role of these critical regulatory enzymes.

Targeting enzymes that control chromatin structure and topography has been an extremely valuable tool in cancer therapy. A wide variety of general and specific small-molecule inhibitors targeted toward HDACs are currently in clinical trials and are used as therapies for both solid and hematological tumors (Bolden et al., 2006). At therapeutic doses, histone deacetylase inhibitors (HDIs) not only cause cell-cycle-dependent DNA damage but also affect DNA repair, which sensitizes cells to ionizing radiation (IR), topoisomerase inhibitors, and cisplatin (Baschnagel et al., 2009; Marchion et al., 2004; Suzuki et al., 2009). However, the molecular mechanism for inefficient DNA repair following HDI treatment is still not clear. Given the high levels of histone acetylation that accumulate in the context of these inhibitors, it is reasonable to assume that disruption of chromatin structure may contribute to cell death. As more selective HDAC inhibitors are moving into clinical trials, it is important to elucidate the function of individual HDACs to design better and more specific drugs for cancer therapy and to understand the mechanism(s) of action or side effects.

Hdac3, a class I HDAC, associates with the nuclear hormone corepressors NCOR and SMRT (Codina et al., 2005) and is generally thought of as a locus-specific corepressor that is recruited to promoters to repress genes regulated by nuclear hormone receptors and other transcription factors (Jones and Shi, 2003). In yeast, Snt1 and Hos2 have features of NCOR/SMRT and Hdac3, respectively (Pijnappel et al., 2001). This suggests a more ancestral and fundamental role of these proteins perhaps in the cell cycle, and that this machinery is also used for gene-specific transcriptional regulation. In agreement with this hypothesis, conditional deletion of *Hdac3* in mouse models demonstrated that murine embryonic fibroblasts (MEFs) required *Hdac3* for cell viability (Bhaskara et al., 2008). The observed apoptosis was associated with an impaired S phase progression and DNA double-strand breaks, rather than altered transcriptional programs (Bhaskara et al., 2008). The DNA damage was blocked when cells were taken out of the cell cycle by serum starvation, which suggested that *Hdac3* acts during the S phase (Bhaskara et al., 2008). We propose that the cell-cycle functions of HDAC3 and its regulatory factors NCOR and SMRT may be the ancestral role and that disruption of these cell-cycle functions may have dramatic consequences for the regulation of chromatin structure and genomic stability. These roles may impact the usefulness of HDAC3 as a therapeutic target in cancer and other diseases.

RESULTS

Hdac3 Function Is Required for Efficient DNA Repair

The inactivation of *Hdac3* resulted in increased sensitivity of quiescent MEFs to ionizing radiation, suggesting a defect predominantly in nonhomologous end joining (NHEJ)-mediated repair in these cells (Bhaskara et al., 2008). To test whether these defects were due to altered DNA repair functions or due to altered histone modifications and the ensuing changes in chromatin structure, we examined whether the inactivation of *Hdac3* increases the sensitivity of *Hdac3*-null cells to other DNA-damaging agents. For this purpose, we treated $Hdac3^{FL/+}$ and $Hdac3^{FL/-}$ MEFs carrying a tamoxifen-inducible *ER-Cre* allele with either increasing concentrations of doxorubicin or cisplatin 48 hr after the addition of 4-hydroxytamoxifen to inactivate *Hdac3*. Doxorubicin inhibits topoisomerase II (Swift et al., 2006) and triggers S phase-associated DNA double-strand breaks that are repaired by the homologous recombination (HR) pathway, whereas cisplatin crosslinks DNA to form intrastrand adducts (Siddik, 2003). Inactivation of *Hdac3* increased the sensitivity of MEFs to doxorubicin (Figure 1A) and cisplatin (Figure 1B), suggesting that in the absence of *Hdac3*, these DNA repair pathways are inefficient.

Given that *Hdac3* deletion appeared to affect two independent types of DNA repair, we examined whether Hdac3 plays a role in the two major NHEJ and HR double-strand-break repair pathways. We employed a chromosomally integrated reporter allele system established in HEK293 cells (Figures 1C and 1D) and used siRNAs to deplete the endogenous levels of HDAC3 (Figure 1E) prior to cutting the reporter site with the I-*Sce*1 homing endonuclease. The efficiency of rejoining I-*Sce*1-cleaved sites was measured using quantitative PCR for NHEJ and by flow cytometry for reconstituted GFP expression for HR. In both cases, the reduction in Hdac3 levels caused a 50%–60% decrease in DNA repair (Figures 1F and 1G), indicating that Hdac3 is essential for efficient NHEJ- and HR-mediated repair.

Although Hdac3 has been linked to NHEJ due to its association with the SMRT/Ku70 complex (Yu et al., 2006), our DNA damage sensitivity and repair data suggested that *Hdac3* loss affects DNA repair by targeting an element that is common to multiple types of DNA repair. Moreover, Hdac3 is not recruited to the sites of double-strand breaks following IR treatment (see Figure S1 available online), nor did its loss affect the localization of other members of the DNA damage response (Rad50, Brca1, Mdc1, and Mre11; data not shown). One of the key histone modifications that contributes to the DNA damage response, the first step in double-strand-break repair, is H3K9 trimethylation (H3K9me3), which recruits the histone acetyltransferase Tip60 (Sun et al., 2009) and other factors involved in the damage response (e.g., HP1β; Ayoub et al., 2008). Therefore, we tested whether siRNA targeting of *HDAC3* would alter histone acetylation at the site of an integrated reporter. Chromatin immunoprecipitation employing anti-H3K9,K14ac showed that histone acetylation was increased at the substrate locus at a level consistent with global changes in H3K9,K14ac (see below), along with a concomitant decrease in H3K9me3 (Figure 1H), suggesting that global changes in histone modifications could contribute to the defects in DNA repair.

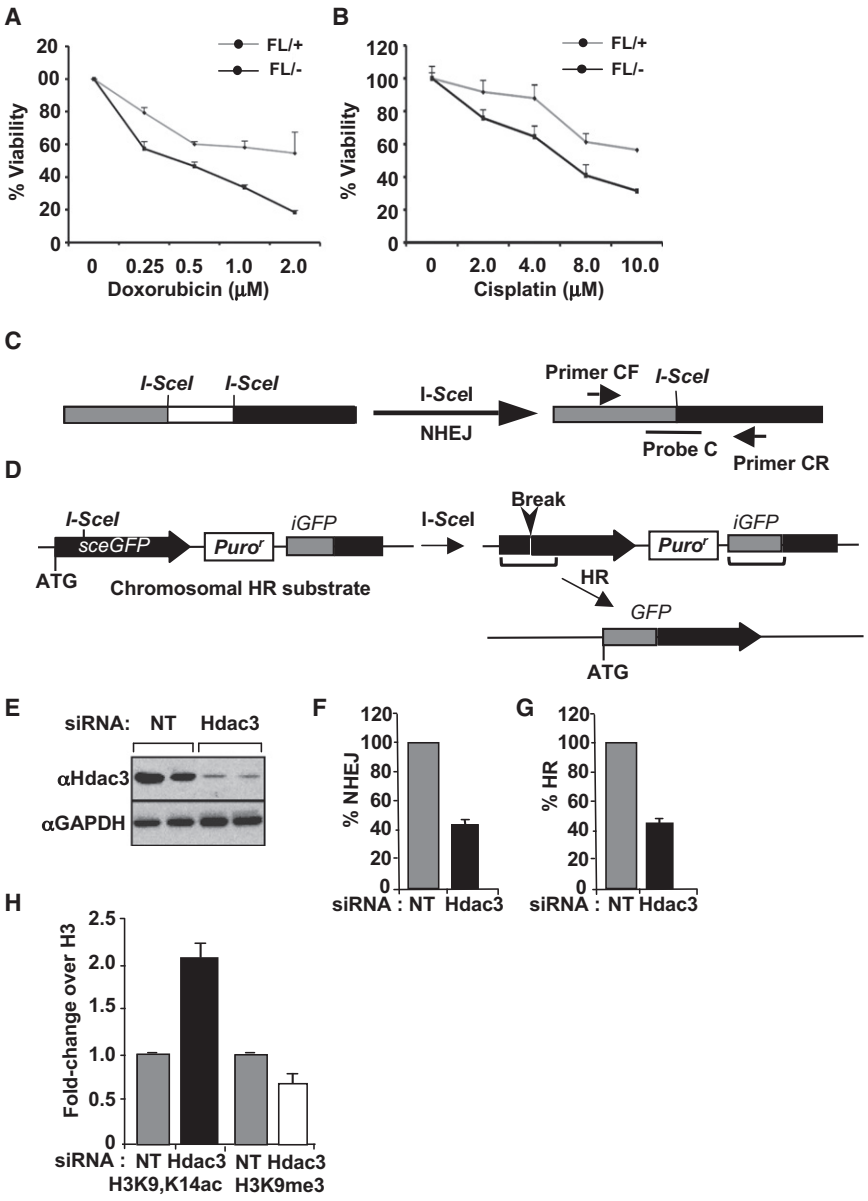

Figure 1. Loss of Hdac3 Impairs DNA Repair

(A and B) MEFs (*Hdac3*$^{FL/+}$ and *Hdac3*$^{FL/-}$) were treated with 0.1 μM tamoxifen for 48 hr and then treated with increasing concentrations of either doxorubicin (A) or cisplatin (B) and cell viability was measured with the WST-1 assay. Values in the graphs represent means ± SD of triplicate samples and the experiment was repeated at least twice.

(C) A schematic representation of the NHEJ substrate (left), the product formed (right), and the position of real-time PCR primers used to detect the repaired product (Zhuang et al., 2009).

(D) The reporter cassette used for HR detection is shown schematically. Upon induction of I-*Sce*1, gene conversion reconstitutes active GFP. The repaired GFP was then measured by FACS analysis.

(E) Western blot analysis of Hdac3 following nontargeting (NT) or Hdac3 siRNA transfection in 293T cells. GAPDH is shown as a loading control.

(F and G) Chromatin-based repair assays performed in 293T cells following knockdown of *Hdac3* to measure the efficiency of NHEJ using quantitative PCR (F) and HR using FACS (G). The values shown in (F) and (G) are the means ± SEM.

(H) Chromatin immunoprecipitation analysis of H3K9,K14ac and H3K9me3 at the NHEJ substrate before and after siRNA suppression of *Hdac3*. Quantitative PCR was used to compare the effects of nontargeting and Hdac3 siRNAs, and the graph shows the average of the relative levels of H3K9,K14ac ± SD.

See also Figure S1.

Inactivation of *Hdac3* Alters Chromatin Structure and Decreases Global Heterochromatin

H3K9me3 is one of the best marks of heterochromatin. The decrease in H3K9me3 upon siRNA-mediated suppression of HDAC3 or Hdac3 deletion in the liver (Figure 1H; see below) prompted us to use the *Albumin-Cre* transgene to delete *Hdac3* in vivo to examine chromatin structure. Initially, we used transmission electron microscopy to examine the nuclei from *Alb-Cre:Hdac3*$^{+/-}$ and *Alb-Cre:Hdac3*$^{-/-}$ postnatal day 17 (p17) livers (Figure 2A). As expected, in control nuclei the electron-dense heterochromatin was found at the nuclear periphery (Figure 2A). In contrast, *Alb-Cre:Hdac3*$^{-/-}$ p17 liver nuclei showed a significant decrease in the amount of heterochromatin, especially at the periphery (Figure 2A; note that the residual electron-dense material remaining is consistent with the presence of nucleoli). A similar result was obtained by enumerating the Hoechst staining of heterochromatic foci that are evident in fluorescence microscopy in mouse cells. *Alb-Cre:Hdac3*$^{-/-}$ liver nuclei showed significantly fewer foci (Figure 2B). Moreover, when cell fractionation was used to isolate chromatin, immunoblot analysis demonstrated that *Alb-Cre:Hdac3*$^{-/-}$ hepatocytes contained roughly 2-fold less HP1β on chromatin (Figure 2C). At the gene-specific level, we used chromatin immunoprecipitation to examine H3K9,K14ac at the *p53* locus (Su et al., 2009). Inactivation of *Hdac3* caused the accumulation of acetylated H3K9,K14 at the promoter, upstream of the promoter, within intron 1, and within the body of the gene (Figure S1), which is consistent with global changes in chromatin structure and histone modifications. Thus, *Hdac3* is required for maintaining chromatin structure in vivo.

Given the reduction in heterochromatin, we used micrococcal nuclease (MNase) digestion to examine nucleosomal compaction. Digestion of isolated nuclei with increasing concentrations of MNase demonstrated that the bulk chromatin from *Hdac3*$^{-/-}$ hepatocytes was more sensitive to MNase digestion when compared to the chromatin from control hepatocytes (Figure 2D), indicating that global chromatin structure was altered and is more "open" in the absence of *Hdac3*. In addition, we noted

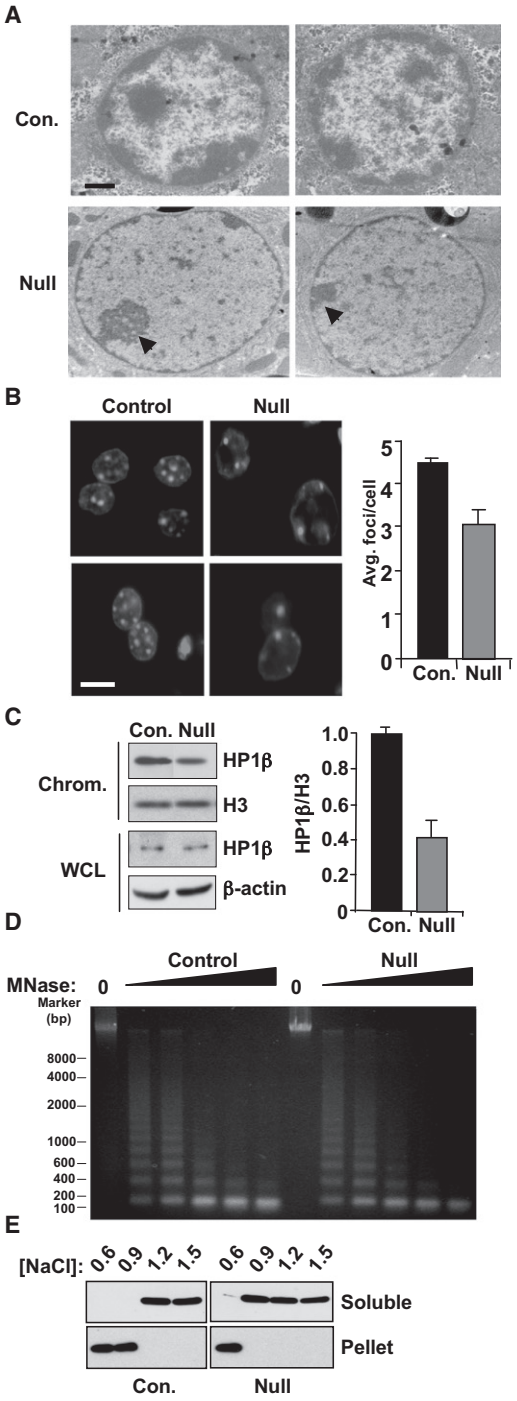

Figure 2. Loss of *Hdac3* Alters Chromatin Structure and Decreases Heterochromatin

(A) Histological sections prepared from control and *Hdac3*-null livers at postnatal day 17 (p17) were used to examine nuclei using electron microscopy. Control hepatocytes contain dense staining of condensed chromatin, whereas *Hdac3*-null cells have decreased amounts of heterochromatin, especially at the nuclear periphery. Arrowheads indicate the RNA-rich nucleoli that remain in the *Hdac3*-null cells. The scale bar represents 4 μm.

(B) Loss of heterochromatic foci upon inactivation of *Hdac3*. Left panels show two examples of histological sections from control and *Hdac3*-null liver stained with Hoechst to detect heterochromatic foci. The scale bar represents 20 μm. The graph at the right shows quantification of foci from at least 100 cells for each sample expressed as the mean ± SEM.

(C) HP1β localization to chromatin is reduced in *Hdac3*-null livers. Chromatin-containing fractions were isolated by cell fractionation, and whole-cell lysates (WCL) or chromatin fractions (Chrom.) were assessed using immunoblot analysis for HP1β, or histone H3 or β-actin as loading controls. Graph shows quantification of the ratio of HP1β to H3 on chromatin from three independent experiments expressed as the mean ± SEM.

(D) Nuclei prepared from *Alb-Cre:Hdac3*$^{+/-}$ control and *Alb-Cre:Hdac3*$^{-/-}$ mice were digested with increasing concentrations of micrococcal nuclease (MNase), and genomic DNA was analyzed using agarose gel electrophoresis. The positions of size markers are shown at the left.

(E) Nucleosome integrity is reduced in *Hdac3*$^{-/-}$ hepatocytes. Cells from *Alb-Cre:Hdac3*$^{+/-}$ control and *Alb-Cre:Hdac3*$^{-/-}$ mice were fractionated and nuclei were extracted with buffer containing the indicated amounts of NaCl (M). Upper panels show the soluble histone H3 and lower panels show the histone remaining in the chromatin pellet.

See also Figure S2.

that the amount of DNA associated with mononucleosomes did not increase with increasing concentrations of MNase, suggesting that the nucleosomal DNA was more accessible in the absence of *Hdac3*. Southern blot analysis of these same samples using major and minor satellite probes or quantitative PCR for these regions showed modest sensitivity without a change in nucleosomal spacing (Figure S2) (Gilbert and Allan, 2001; Sugimura et al., 2010). Given the apparent sensitivity of mononucleosomal DNA to MNase (Figure 2D), we tested the sensitivity of nucleosomes to ionic conditions by extracting histones with differing concentrations of salt. Consistent with prior results (Li et al., 1993), histone H3 was resistant to NaCl concentrations up to 1.2 M in control hepatocytes, but in the absence of *Hdac3*, histone H3 was nearly completely soluble in 900 mM NaCl, suggesting that nucleosome integrity was altered in *Hdac3*$^{-/-}$ hepatocytes.

Structural determinations of the nucleosome show that the basic lysine residues in histone tails can potentially associate with DNA, but more likely mediate contacts with acidic surfaces on adjacent nucleosomes to allow nucleosome compaction and fiber formation (Luger et al., 1997; Luger and Richmond, 1998; Schalch et al., 2005). Therefore, we performed western blot analysis of nuclear extracts prepared from *Alb-Cre:Hdac3*$^{+/-}$ or *Alb-Cre:Hdac3*$^{-/-}$ p17 livers to examine global histone acetylation and methylation marks that neutralize the lysine charges and that regulate chromatin structure. Hdac3 deacetylates H4K5ac and H4K12ac in vitro (Johnson et al., 2002), and loss of *Hdac3* resulted in an accumulation of H4K5ac, H4K12ac, and H4K16ac, as well as H3K9,K14ac, with little effect on the acetylation of other residues (Figure 3) (Knutson et al., 2008). Examination of histone methylation demonstrated that H3K9me3 (Lachner et al., 2001) and H3K79me2 were reduced (Figure 3), whereas H3K4me3, H3K27me3, and H4K20me2 were unaffected (Figure 3).

H4K5ac and H4K12ac are commonly associated with histone deposition onto newly synthesized DNA. Given that hepatocytes are generally quiescent, our liver-specific deletion of *Hdac3* implies that Hdac3 is required for removing these marks during or after DNA synthesis. Therefore, we used *Hdac3*$^{FL/-}$ NIH 3T3 cells infected with adenovirus expressing *Cre* to examine these marks during the cell cycle. Cells were infected with *Adeno-Cre* and synchronized in G_0/G_1 by serum starvation and then

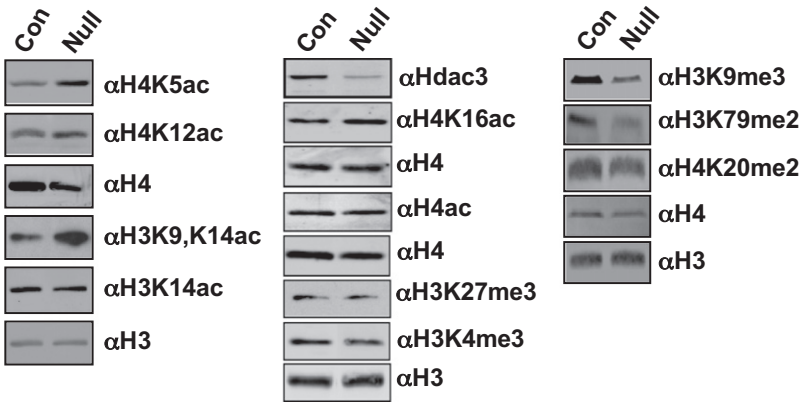

Figure 3. Deletion of *Hdac3* Increases H4K5ac, H4K12ac, and H3K9,K14ac

Western blot analysis of nuclear extracts prepared from p17 *Hdac3*-null hepatocytes to examine histone acetylation and histone methylation levels. H3 and H4 served as loading controls.

released into the cell cycle by the addition of serum to the culture medium. The level of H4K5ac and H4K12ac was then examined using western blot analysis of extracts prepared from cells at various time points after serum addition. After 48 hr of culture in the absence of serum, the percentage of cells in G_0/G_1 approached 90% (Figure S3) and H4K5ac and H4K12ac were reduced to low levels in control cells but remained high in *Hdac3*-depleted cells (Figure 4A). After serum addition, both cultures re-entered the cell cycle, with cells beginning to enter S phase at 12 hr and over 50% of the cells progressing through S phase by 18 hr as measured by BrdU incorporation (Figure S3). At 18 and 24 hr after serum addition, H4K5ac and H4K12ac increased in the control cells, consistent with the acetylation of these residues on newly synthesized histones that are deposited on new DNA (Figure 4A). In cells lacking *Hdac3*, the levels of acetylation of these residues were already high and increased only modestly during S phase (Figure 4A). Whereas H3K9,K14 acetylation has not been linked to histone deposition in mammalian cells in the manner that H4K5ac and H4K12ac have, its levels were low in G_0/G_1 phase control cells and increased during S phase. In the absence of *Hdac3*, H3K9,K14ac was not reduced upon serum starvation, suggesting that acetylation of these residues was not removed after S phase, which could account for the loss of H3K9me3 and reduced heterochromatin in *Hdac3*-null livers (Figures 2 and 3).

To better define the requirements for Hdac3 in the removal of cell-cycle-associated marks, we directly examined H4K5ac in S phase cells, as this is a classical deposition mark. The punctate immunofluorescence pattern of PCNA 18 hr after release from serum starvation was used to identify cells in late S phase, which are characterized by foci of PCNA at the nuclear periphery (Celis and Celis, 1985; Madsen and Celis, 1985; Taddei et al., 1999). Although a general increase in H4K5ac was observed in the absence of *Hdac3* (data not shown), a pronounced increase in H4K5ac was found in late S phase cells (11% of cells in controls versus 57% of *Hdac3*-null cells) (Figure 4B), especially at the nuclear periphery.

Even relatively modest overexpression or reduced expression of histones is sufficient to affect genomic stability by causing DNA double-strand breaks (Gunjan and Verreault, 2003; Olive and Banath, 1995). Given the apparent high level of H4K5ac in the nucleus of *Hdac3*-null cells after S phase (Figures 4A and 4B), we asked what proportion of the total histone H4 is acetylated in the absence of *Hdac3*. Two sequential rounds of immunoprecipitation of lysates prepared from quiescent *Hdac3*-null NIH 3T3 cells were performed using anti-H4K5ac to identify the acetylated histone. Western blot analysis using anti-H4K5ac confirmed that most of the acetylated histone was immunopurified in the first immunoprecipitation (Figure 4C, upper). The total histone H4 that was acetylated at K5 was then determined by comparing the amount of total histone H4 in the immunoprecipitation versus H4 that remained in the supernatant (Figure 4C, lower). For the western blot analysis, one-fifth the amount of the supernatant was loaded as compared to the precipitated H4K5ac. Thus, roughly 15%–20% of the total histone H4 was acetylated at K5 in control cells and 30%–40% was acetylated in the absence of *Hdac3* (Figure 4C).

Hdac3 Is Required for Genomic Stability

Previously, we noted S phase-associated DNA double-strand breaks in *Hdac3*-null cells (Bhaskara et al., 2008). Given the requirement for Hdac3 in removing histone acetylation marks that are added during the S phase of the cell cycle and the links between loss of H3K9me3 and genomic instability, we examined the consequences of inactivation of *Hdac3* to chromosomes as they progress through mitosis. Metaphase spreads were prepared from $Hdac3^{FL/+}$ and $Hdac3^{FL/-}$ MEFs following either Ad-Cre infection or following tamoxifen treatment of MEFs carrying the *ER-Cre* transgene. Both chromosome breaks and gaps were quantified using cytogenetic analysis. Using either Ad-Cre (Figure S4) or ER-Cre to delete *Hdac3* (Figure 5A) led to a 5- to 8-fold increase in the average number of breaks and gaps in metaphase chromosomes when compared to control cells (Figure 5B), indicating a crucial role for Hdac3 in the maintenance of genome stability.

To test whether the DNA damage and genomic instability phenotypes found in MEFs lacking *Hdac3* were recapitulated in vivo, we examined *Alb-Cre:*$Hdac3^{+/-}$ and *Alb-Cre:*$Hdac3^{-/-}$ livers for DNA double-strand breaks using immunofluorescence to detect γH2AX and 53BP1, which localize to sites of DNA double-strand breaks (Iwabuchi et al., 2003). Whereas there was little or no endogenous DNA damage in *Alb-Cre:*$Hdac3^{-/-}$ livers at p17 (data not shown), by p28 the *Hdac3*-null livers displayed an increased number of cells with γH2AX and 53BP1 foci when compared to the control hepatocytes (Figure 5C, 0 Gy panels; see Figure S4 for quantification). Subsequently, we examined DNA repair in *Hdac3*-null hepatocytes at p28 following a nonlethal dose of IR (3 Gy). An increased percentage of cells with a substantial amount of DNA damage was detected both 1 and 6 hr after IR in *Alb-Cre:*$Hdac3^{-/-}$ when compared to the control *Alb-Cre:*$Hdac3^{+/-}$ hepatocytes

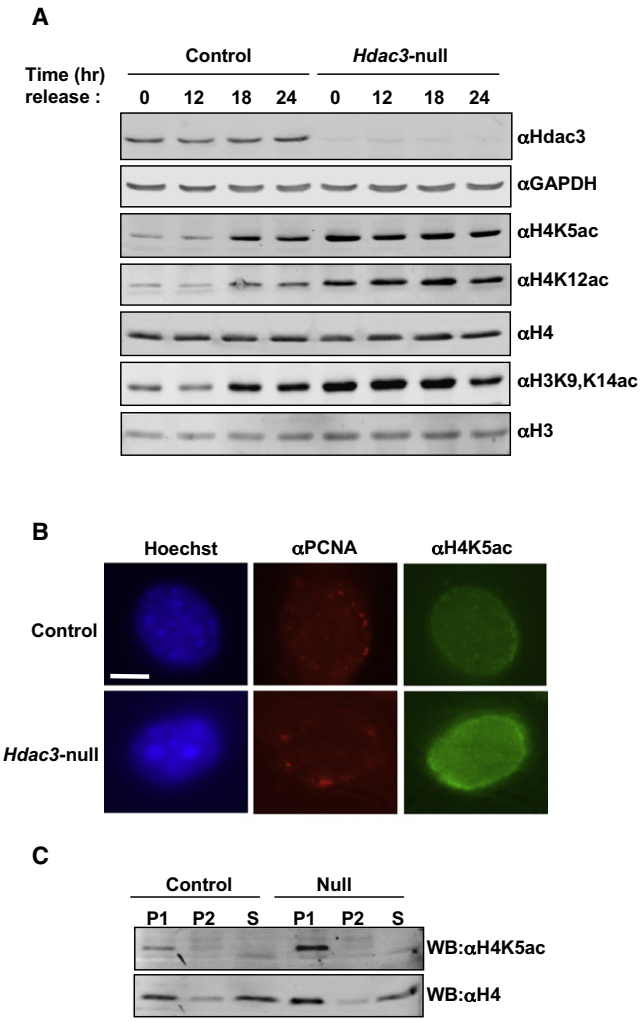

Figure 4. Inactivation of *Hdac3* Increases H4K5 and H4K12 Acetylation in Synchronized Cells

(A) Wild-type NIH 3T3 cells (control) or *Hdac3*$^{FL/-}$ NIH 3T3 cells infected with Ad-Cre for 48 hr (*Hdac3*-null) were cultured in 0.5% serum-containing media for 48 hr. Cells were then transferred to media containing 10% fetal calf serum, and lysates were prepared at the times indicated and analyzed by western blot to measure the levels of the indicated histone modifications. GAPDH served as a loading control.

(B) Immunofluorescence analysis of H4K5ac in S phase cells following release of serum-starved G_o/G_1 cells into regular media for 18 hr. Late S phase cells were identified by the punctate pattern of PCNA staining at the nuclear periphery. Zoomed images of individual nuclei are shown. The scale bar represents 10 μm.

(C) Immunoprecipitation of quiescent control or *Hdac3*-null lysates with anti-H4K5ac and western blot analysis with anti-H4K5ac and anti-H4. P1, first immunoprecipitation; P2, reimmunoprecipitation of the supernatant from P1; S, supernatant from P2.

See also Figure S3.

(Figure 5C). Quantification of 53BP1 foci in ~100 cells from two independent experiments following a 6 hr recovery period revealed that *Hdac3*-null cells have a greater percentage of cells with five to ten foci when compared to the control cells (Figure S4). We also observed DNA damage even after a 24 hr recovery period in some *Alb-Cre:Hdac3*$^{-/-}$ hepatocytes, whereas control hepatocytes had repaired the damage caused by IR treatment (data not shown).

Hdac3-Null Livers Develop Hepatocellular Carcinoma

Analysis of gene expression data obtained previously from *Alb-Cre:Hdac3*$^{-/-}$ livers at p28 identified an upregulation of genes that belong to the p53 network (Figure S4), suggesting the presence of DNA damage. Likewise, quantitative RT-PCR analysis revealed an upregulation of miRNAs regulated by p53 in *Hdac3*-null livers (Figure S4), which is also consistent with the activation of a DNA damage response (Rokhlin et al., 2008). In addition, hepatocellular carcinoma (HCC) progression markers, such as γ-glutamyltranspeptidase1 (Pavesi et al., 1989) and insulin-like growth factor II (Qiu et al., 2008), were upregulated in the microarray analysis of *Alb-Cre:Hdac3*$^{-/-}$ livers by 2.2- and 2.7-fold, respectively (Knutson et al., 2008). These data, coupled with the observed genomic instability, prompted us to age cohorts of 20 control and 20 *Alb-Cre:Hdac3*$^{-/-}$ mice. By 15–16 weeks of age, the livers were very pale due to the dramatic accumulation of neutral lipids and fat caused by inactivation of *Hdac3* (Knutson et al., 2008) and contained "white nodules" when examined by gross morphology (Figure 6A). These nodules were encapsulated with a fibrous lining that positively stained with Massion's trichrome (data not shown) and appeared to be benign "adenoma-like" structures with the cytoplasm of the cells filled with microvesicular fluid and an abundance of mitochondria (Figure 6A and data not shown). By 8–10 months of age, most of the mice began to show signs of distress, and necropsy identified the presence of tumors in the liver. The experiment was humanely terminated for all mice by 14 months of age (Figure 6B). Pathological analysis indicated that 20 of 20 mice succumbed to low-grade HCC at a mean age of 10.2 months (Figure 6B). Immunohistochemical staining for Hdac3 confirmed that the tumors lacked expression of *Hdac3* (Figure 6C) and Ki67 staining confirmed a high proliferative index in the tumors (Figure 6D). The HCC displayed a loss of normal architecture, a trabecular patterning of cells, a lack of ductal morphology, and very disorganized features (Figure 6D).

The loss of genomic stability and the impaired response to DNA damage suggested that a high mutation rate stimulated the development of HCC (Figures 1, 5, and 6). To begin to assess what pathways were involved in the formation of HCC, we performed gene expression analysis using cDNA microarrays (Figure 7A). In the array data, we noted the enhanced expression of *c-Myc*, a commonly overexpressed oncogene, which was confirmed using quantitative RT-PCR (Figure 7B). Signatures consistent with activation of the Ras pathway and impairment of the p53 pathway were also identified in this analysis (Figure 7A). The Wnt pathway has been identified as a key regulatory node in human HCC and we also noted that this pathway was affected in the *Hdac3*-null tumors. Therefore, we examined β-catenin localization using both cell fractionation and immunohistochemical staining. As early as p28, we found increased amounts of β-catenin localized to the nucleus and there was prominent nuclear localization of β-catenin in the *Hdac3*-null HCCs (Figures 7B and 7C), confirming that this oncogenic pathway was upregulated in this mouse model of HCC.

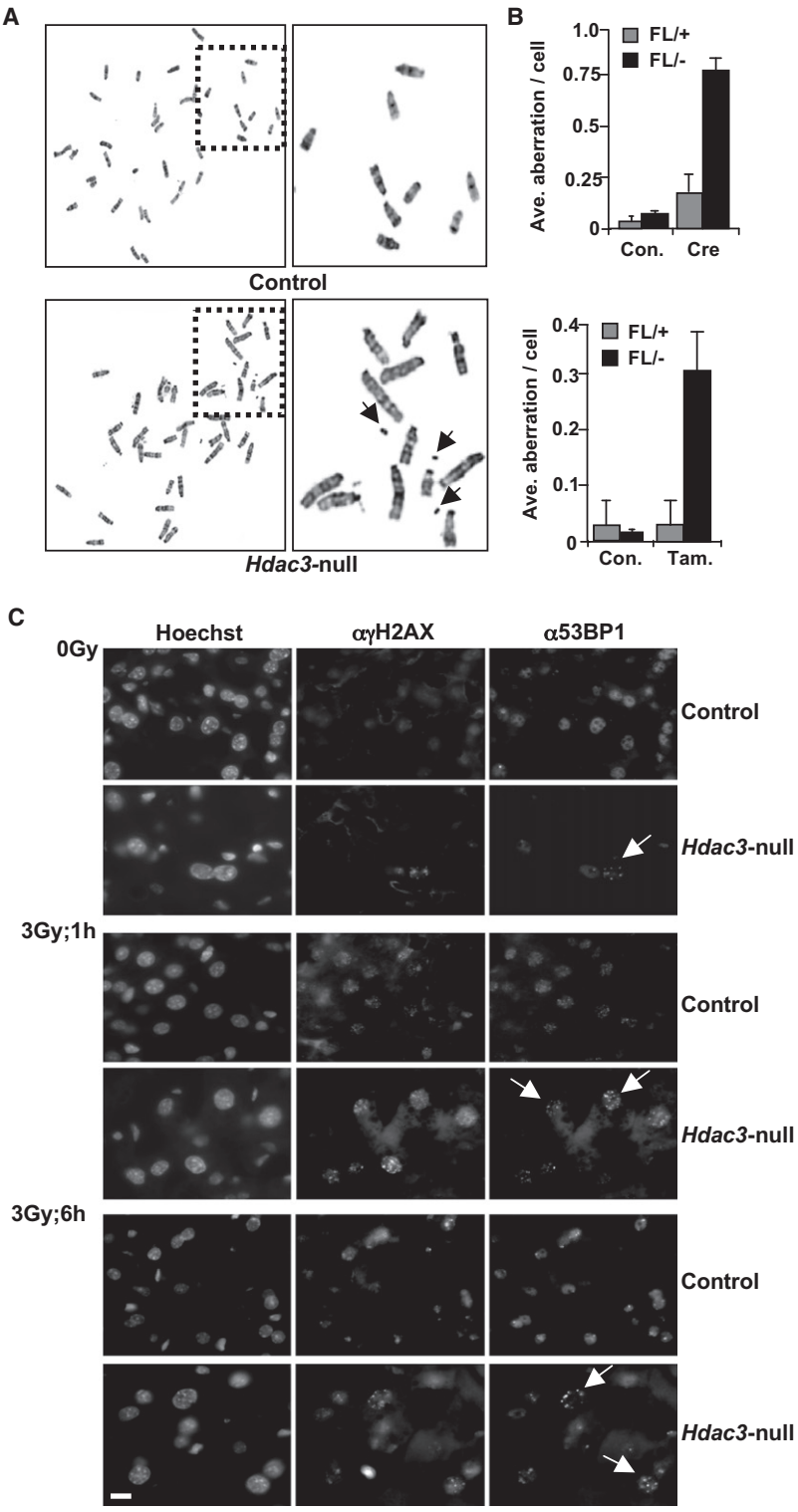

Figure 5. Loss of *Hdac3* Causes Genomic Instability

(A) Metaphase spreads prepared from *ER-Cre:Hdac3*$^{FL/+}$ and *ER-Cre:Hdac3*$^{FL/-}$ MEFs treated with either vehicle (top) or tamoxifen (bottom). Magnified views of a group of chromosomes outlined in the left panels are shown in the right panels. Arrows indicate broken pieces of chromosomes.

(B) The numbers of breaks and gaps observed in control or null MEFs (Ad-Cre- or tamoxifen-treated *ER-Cre:Hdac3*$^{FL/-}$) were quantified, and the data in the graphs represent the mean ± SD. The numbers of breaks and gaps per cell were calculated from two different MEF preparations, in which a total of 50 cells were counted in each preparation.

(C) DNA repair is impaired in *Hdac3*-null livers. *Hdac3*-null hepatocytes are defective in DNA repair. Mice were irradiated with a 3 Gy dose of IR, and frozen sections of livers collected immediately or 1 or 6 hr later were prepared for immunofluorescence analysis of γH2AX and 53BP1. Arrows indicate *Hdac3*-null nuclei with 53BP1 foci. The scale bar represents 20 μm.

See also Figure S4.

NCOR1 Is Downregulated in HCC and NCOR and SMRT Regulate Global Histone Acetylation

Analysis of *HDAC3* mRNA levels in four independent human HCC data sets from the Gene Expression Omnibus (GEO) database indicated that *HDAC3* was reduced in some cases (Figure 8; Figure S5). *HDAC3* is highly expressed in cycling cells (e.g., in the crypt regions of the colonic epithelium) (Spurling et al., 2008; Wilson et al., 2006), so comparing quiescent normal tissue to cycling cancer cells may underestimate the level of its loss of expression. Nevertheless, in the largest data set, *HDAC3* levels were reduced by 1.5-fold in 13% of the cases and over 2-fold in 3.3% of the cases as compared to normal controls (data not shown and Figure 8A). There was no association with hepatitis C or hepatitis B viral infection or survival (data not shown). Given that HDAC3 is dormant until activated by association with NCOR or SMRT (Guenther et al., 2001) and that it is recruited to chromatin through association with other factors, we probed the GEO HCC data sets for changes in expression of the 57 direct interaction partners of HDAC3 identified in the Human Protein Reference Database (Table S1). Four of these genes (*STAT3*, *GTF2I*, *GCM1*, and *NCOR1*) showed reduced expression in HCC. *NCOR1* is not only downregulated but is also located on a region of chromosome 17p that is deleted in human HCC (Xu et al., 2001). The levels of *NCOR1* were reduced by 2-fold or greater in nearly one-third of HCC samples in the largest data set (Figure 8A) and were similarly downregulated in the majority of the samples in smaller HCC gene expression data sets (Figure S6). Using immunohistochemistry to detect nuclear NCOR1, we found that two-fifths of the human HCCs tested had reduced levels of NCOR1 (Figure 8B), which is consistent with the mRNA expression results.

Given that NCOR/SMRT directly control HDAC3 functions (Guenther et al., 2001), we used siRNAs to probe the

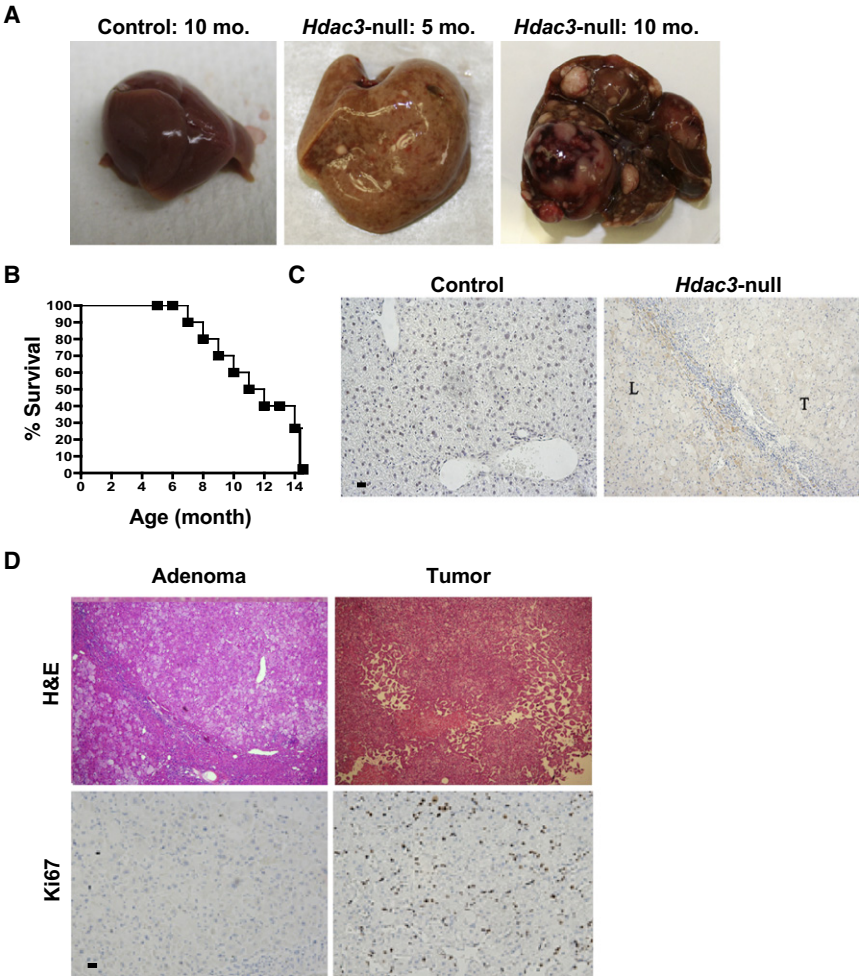

Figure 6. Loss of *Hdac3* Leads to Hepatocellular Carcinoma

(A) Representative livers of 5-month-old (middle) and 10-month-old (right) *Alb-Cre:Hdac3*$^{-/-}$ mice.

(B) Survival plot for *Alb-Cre:Hdac3*$^{-/-}$ mice. Heterozygous mice showed no mortality within this time frame.

(C) Immunohistochemistry using anti-Hdac3 shows that normal hepatocytes express Hdac3 (left), whereas *Alb-Cre:Hdac3*$^{-/-}$ mice lack Hdac3 both in the tumor and surrounding tissue. T, tumor; L, liver. The scale bar represents 60 μm.

(D) Hematoxylin and eosin-stained histological sections (H&E; top) and immunohistochemistry for Ki67 (bottom) from 10-month-old *Alb-Cre:Hdac3*$^{-/-}$ mice. The scale bar represents 60 μm. See also Figure S5.

requirements for these HDAC3 cofactors in the regulation of histone acetylation. In HeLa cells that express both family members, depletion of either NCOR or SMRT alone had only modest effects on global histone acetylation (data not shown). Targeting both family members together caused a small increase in H4K5ac (Figure 8C). However, even though NCOR/SMRT levels were only reduced by about 50%, there was a significant accumulation in the levels of global H4K5ac in both HeLa cells (Figure 8C) and NIH 3T3 cells (Figure S6B). These increases in histone acetylation were associated with a decrease in the levels of HDAC3 detected in both HeLa and NIH 3T3 cells (Figure 8C; Figure S6C). Immunofluorescence using anti-PCNA to identify S phase cells demonstrated a 5-fold increase in the number of cells with high levels of H4K5ac at the nuclear periphery in late S phase cells targeted with siRNAs to both cofactors (Figure 8D; Figure S6C). Given this alteration in histone marks, we examined these cells for DNA double-strand breaks using anti-53BP1. Cells depleted of *NCOR1* and *SMRT* showed a dramatic increase in the number of cells with greater than ten foci (Figure 8E; Figure S6D). Collectively, these results show that the NCOR/SMRT/HDAC3 axis is required for removing histone marks globally and maintaining genomic stability.

DISCUSSION

The increase in acetylation of H4K5, H4K12, H4K16, and H3K9,K14 that was observed upon inactivation of *Hdac3*, along with the concomitant loss of H3K9me3, provides a likely mechanism for the failure to maintain chromatin structure in *Hdac3*-null mice (Figure 2). H4K5ac and H4K12ac are associated with histone deposition (Sobel et al., 1995), especially in heterochromatic regions that are replicated late in S phase (Taddei et al., 1999), and this pattern was accentuated in the absence of *Hdac3* or when NCOR/SMRT were targeted using siRNAs (Figures 4 and 8). The removal of these marks is required for propagation of heterochromatin in yeast (Zhou et al., 2009), which suggests that the accumulation of these marks (and the reduced levels of H3K9me3) may be the underlying cause for the reduction in heterochromatin in the *Hdac3*-null livers. Indeed, loss of H3K9me3 impaired the DNA damage response, and the inactivation of the murine H3K9 methyltransferases or mutation of HP1β caused genomic instability, defects in double-strand-break repair, and an increased tumor risk (Aucott et al., 2008; Kondo et al., 2008; Luijsterburg et al., 2009; Peters et al., 2001; Sun et al., 2009). This suggests that the failure to maintain a normal chromatin structure underlies the *Hdac3*$^{-/-}$-associated defects in two distinct types of DNA repair (NHEJ and HR), and in genomic stability (Figures 1 and 5), which ultimately led to tumor development (Figure 6).

The siRNA-mediated knockdown of NCOR/SMRT, like deletion of *Hdac3*, caused the accumulation of histone deposition marks, suggesting that these Hdac3-activating factors also play an intrinsic role during the cell cycle. NCOR and SMRT were initially identified as transcriptional corepressors associated with nuclear hormone receptors (Chen and Evans, 1995; Horlein et al., 1995; Karagianni and Wong, 2007), as well as with a variety of DNA-binding factors (Perissi et al., 2004). However, the function of these corepressors during the cell cycle

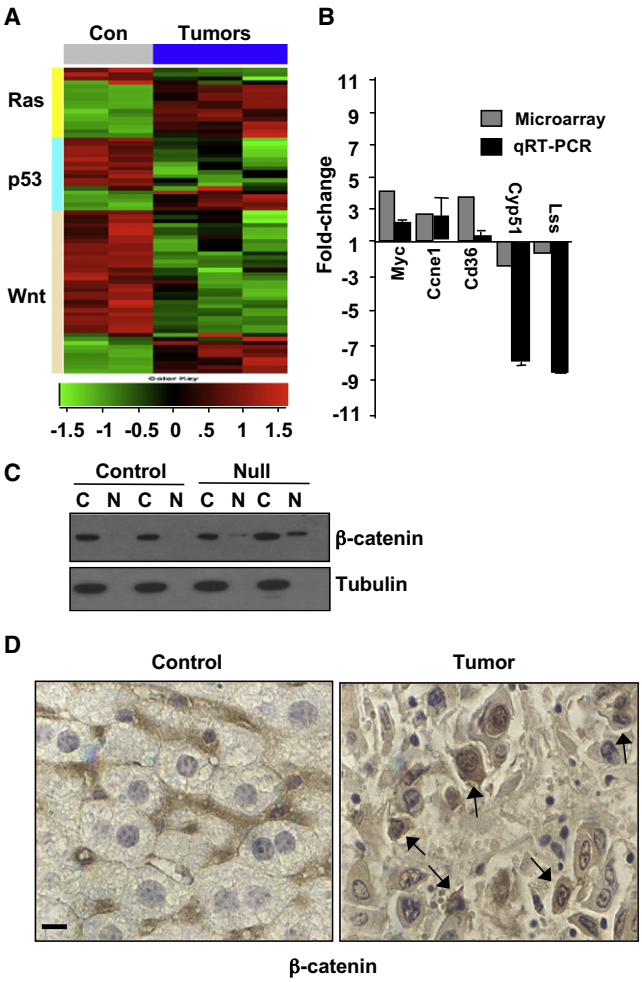

Figure 7. β-Catenin Is Misregulated in *Hdac3*-Null HCC

(A) Heat map of selected genes from a cDNA microarray analysis of control liver and *Hdac3*-null HCCs. The levels of mRNAs expressed from genes associated with the Ras, p53, and Wnt pathways are depicted as green (low) or red (high), where black indicates no change.

(B) Quantitative RT-PCR confirmation of the microarray results. The graph shows the expression levels of the indicated genes obtained on the microarrays and from quantitative RT-PCR as the average fold increase or decrease over controls that were set to 1 ± SD.

(C) β-catenin is mislocalized in *Hdac3*-null livers. Control and p28 *Hdac3*-null hepatocytes were separated into cytoplasmic (C) and nuclear (N) fractions and β-catenin was detected by immunoblot. Tubulin was used to monitor cytoplasmic contamination of nuclei.

(D) β-catenin is nuclear in *Hdac3*-null HCC. Immunohistochemistry was used to determine the cellular localization of β-catenin (brown tint). Nuclei were counterstained with hematoxylin (blue tint). Arrows indicate cells with prominent nuclear β-catenin. The scale bar represents 20 μm.

See also Table S1.

may represent the ancestral activity of these complexes. We speculate that during evolution this cell-cycle machinery was recruited in higher organisms to regulate gene expression patterns in a cell-type-specific manner (e.g., in response to nuclear hormones) or to form heterochromatin to more permanently silence gene expression.

Although HDAC3 has been suggested to be overexpressed in colorectal carcinoma (Spurling et al., 2008; Wilson et al., 2006), it is not amplified at the DNA level. In addition, *HDAC3* is expressed at higher levels in the proliferating cells of the colonic crypts, which might suggest that its levels are higher in colorectal carcinoma because the cells are cycling. Conversely, it is notable that *HDAC3* lies within a region of chromosome 5q31.3 that is frequently deleted in breast cancer (Johannsdottir et al., 2006) and myelodysplastic syndromes (Ebert, 2009). Intriguingly, *NCOR1* lies in a region of chromosome 17 that is frequently deleted in HCC (Mahlknecht et al., 1999), and an analysis of expression profiles indicated that downregulation of *NCOR1* expression is common in a subset of human HCC (Figure 8A; Figure S6). Our data are consistent with the inactivation of the HDAC3/NCOR/SMRT axis, possibly contributing to a subset of human cancer by allowing the increase of histone acetylation during the S phase, leading to DNA damage and further accumulation of mutations.

Nearly all nontargeted cancer therapeutics (i.e., those that do not target a mutant protein that initiates a cancer) develop a therapeutic window by acting on cycling cells to cause DNA damage (Ashwell and Zabludoff, 2008; Lieberman, 2008). However, one side effect is that these agents, when given at too high a dose or for too long, also cause genomic instability in normal cells, leading to therapy-associated secondary cancers. Our results raise this possibility for HDIs, all of which currently target HDAC3. However, compounds such as SAHA appear to be well tolerated, possibly owing to their short half-life in vivo (Butler et al., 2000). That is, SAHA may cause S phase-associated DNA damage for those cancer cells in S phase during the 4–6 hr window in which the daily dose of SAHA is active, but only cause mild problems for the majority of normal cells that are not cycling. In addition, normal cells that are proliferating, such as in the gastrointestinal tract and in the bone marrow, can either repair the DNA damage or their chromatin is "reset" after the SAHA is metabolized. Thus, we predict that although continuous inhibition of Hdac3 is detrimental (e.g., Figure 6), transient inhibition, even when frequently repeated, may be safe.

EXPERIMENTAL PROCEDURES

See Supplemental Experimental Procedures for additional methods used.

Mice

Mice harboring either a conditional floxed (FL) allele or a null (–) allele were created as described previously (Knutson et al., 2008). To create liver-specific *Hdac3* knockout mice, mice with a floxed or a null allele were crossed to transgenic mice expressing *Alb-Cre* (Knutson et al., 2008) to obtain *Alb-Cre:Hdac3*$^{+/-}$ and *Alb-Cre:Hdac3*$^{-/-}$ offspring mice. All experiments using mice were approved by the Vanderbilt University Institutional Animal Care and Use Committee.

DNA Repair Assays

DNA repair assays were performed using HEK293 cells engineered with integrated reporters for both types of double-strand-break repair (Zhuang et al., 2009). Briefly, cells (1×10^5) were transfected twice with *HDAC3* siRNA using Oligofectamine (Invitrogen). pCMV-*I-Sce*1 or the control vector was transfected into the cells using FuGene 6 (Roche). The cells were either analyzed by two-color FACS analysis to examine homologous recombination or PCR was used to determine the rate of NHEJ-mediated repair (see Supplemental Experimental Procedures for primer sequences).

Transmission Electron Microscopy

Liver tissue was minced into fine pieces and fixed in 2.5% glutaraldehyde in 0.1 M cacodylate buffer at room temperature for 1–2 hr. Samples were then washed in 0.1 M cacodylate buffer and treated with 1% aqueous osmium

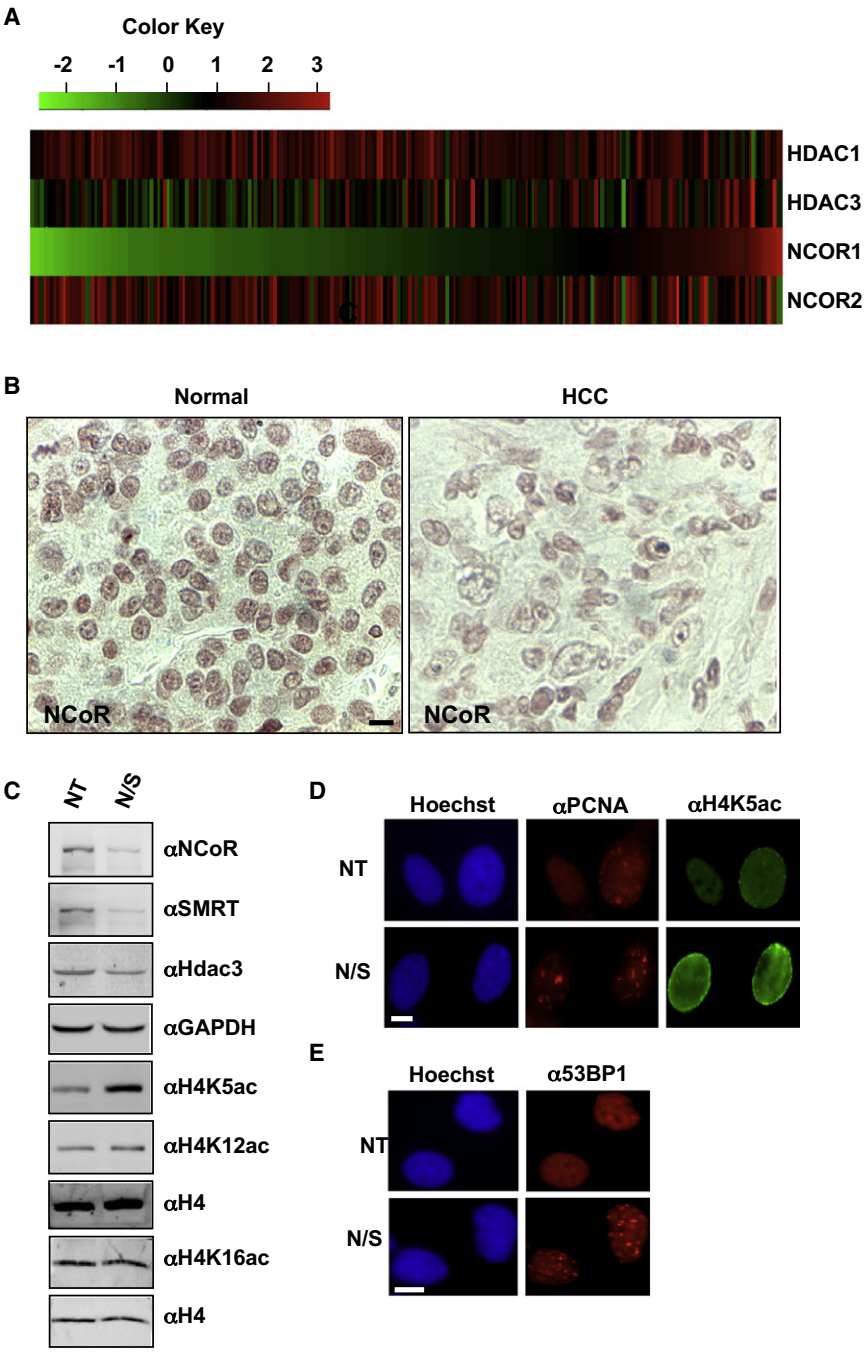

Figure 8. *NCOR1* Is Downregulated in Human HCC and siRNA Targeting of NCOR and SMRT Causes DNA Damage

(A) Heat map representation of the analysis of *NCOR1*, *NCOR2*, *Hdac3*, and *Hdac1* mRNA levels in human HCC samples (GEO 5975 data set). Green depicts low expression relative to the mean of control samples and red indicates higher expression. A 2-fold cutoff was used to define a significant change.

(B) NCOR1 is downregulated in a subset of human HCCs. Immunohistochemical staining was used to detect NCOR1 in human HCC or normal matched surrounding tissue (brown stain). Cells were counterstained with hematoxylin (blue tint). The scale bar represents 20 μm.

(C) HeLa cells were transfected with either nontargeting (NT) or NCOR/SMRT siRNA (N/S). Whole-cell lysates were analyzed for histone modifications using western blot.

(D) Immunofluorescence analysis of H4K5 acetylation in HeLa cells transfected with either nontargeting (NT) or NCOR/SMRT siRNA (N/S). The scale bar represents 10 μm. S phase cells were identified by the punctate pattern of PCNA staining.

(E) Immunofluorescence analysis of 53BP1 in HeLa cells transfected with either nontargeting siRNA (NT) or NCOR/SMRT siRNA (N/S). The scale bar represents 10 μm.

See also Figure S6.

tetraoxide. Tissues were then washed, dehydrated, and embedded in Spurr resin. Thin sections (100 nm) were viewed with an FEI CM-12 transmission electron microscope operated at 80 KeV.

Gene Expression Analysis of Human HCC Samples

Four HCC and normal control experiments (GSE14323, GSE6764, GSE6222, and GSE5975) were selected from the Gene Expression Omnibus database (http://www.ncbi.nlm.nih.gov/geo) (Barrett et al., 2009). The description of this analysis is elaborated in Supplemental Experimental Procedures. For GSE6764 (Wurmbach et al., 2007), we compared the normal liver samples with HCC samples of different stages. For GSE6222 (Liao et al., 2008), we excluded the HuH7 cell line data. GSE1898 was excluded from this analysis due to variations in the probe sets. Expression data generated from murine tumors lacking Hdac3 are found in GSE22457.

Protein Analyses

For preparation of whole-cell protein extracts, the cell pellet was washed with PBS and sonicated in RIPA buffer (0.5% Triton X-100, 0.5% deoxycholic acid, and 0.5% SDS in PBS) with protease inhibitors (0.5 mM PMSF, 2 μg/μl leupeptin, and 15 μg/μl aprotinin) prior to western analyses. Antibodies used and the preparation of nuclear extracts are described in Supplemental Experimental Procedures.

ACCESSION NUMBERS

Expression data generated from murine tumors lacking *Hdac3* have been deposited in the Gene Expression Omnibus database under accession number GSE22457.

SUPPLEMENTAL INFORMATION

Supplemental Information includes six figures, one table, and Supplemental Experimental Procedures and can be found with this article online at doi:10.1016/j.ccr.2010.10.022.

ACKNOWLEDGMENTS

We thank all the members of the Hiebert lab for helpful discussions, reagents, and advice. We thank the Vanderbilt Imaging, Human Tissue Acquisition and Pathology, and Functional Genomics Shared Resources for services and support. We thank Drs. Nick Gilbert and James Allan for providing plasmids containing the major and minor satellite probes. This work was supported by The T.J. Martell Foundation, The Robert J. Kleberg, Jr. and Helen C. Kleberg Foundation, National Institutes of Health grants (R01-CA64140, R01-CA77274, and R01-CA109355), and core services performed through Vanderbilt Digestive Disease Research grant NIDDK P30DK58404 and Vanderbilt-Ingram Cancer Center support grant NCI P30CA68485. S.B. was supported by a fellowship (1F32CA138091-01) from the NCI.

Received: January 14, 2010
Revised: June 16, 2010
Accepted: August 23, 2010
Published: November 15, 2010

REFERENCES

Ashwell, S., and Zabludoff, S. (2008). DNA damage detection and repair pathways—recent advances with inhibitors of checkpoint kinases in cancer therapy. Clin. Cancer Res. *14*, 4032–4037.

Aucott, R., Bullwinkel, J., Yu, Y., Shi, W., Billur, M., Brown, J.P., Menzel, U., Kioussis, D., Wang, G., Reisert, I., et al. (2008). HP1-β is required for development of the cerebral neocortex and neuromuscular junctions. J. Cell Biol. *183*, 597–606.

Ayoub, N., Jeyasekharan, A.D., Bernal, J.A., and Venkitaraman, A.R. (2008). HP1-β mobilization promotes chromatin changes that initiate the DNA damage response. Nature *453*, 682–686.

Barrett, T., Troup, D.B., Wilhite, S.E., Ledoux, P., Rudnev, D., Evangelista, C., Kim, I.F., Soboleva, A., Tomashevsky, M., Marshall, K.A., et al. (2009). NCBI GEO: archive for high-throughput functional genomic data. Nucleic Acids Res. *37*, D885–D890.

Baschnagel, A., Russo, A., Burgan, W.E., Carter, D., Beam, K., Palmieri, D., Steeg, P.S., Tofilon, P., and Camphausen, K. (2009). Vorinostat enhances the radiosensitivity of a breast cancer brain metastatic cell line grown in vitro and as intracranial xenografts. Mol. Cancer Ther. *8*, 1589–1595.

Bhaskara, S., Chyla, B.J., Amann, J.M., Knutson, S.K., Cortez, D., Sun, Z.W., and Hiebert, S.W. (2008). Deletion of histone deacetylase 3 reveals critical roles in S phase progression and DNA damage control. Mol. Cell *30*, 61–72.

Bolden, J.E., Peart, M.J., and Johnstone, R.W. (2006). Anticancer activities of histone deacetylase inhibitors. Nat. Rev. Drug Discov. *5*, 769–784.

Butler, L.M., Agus, D.B., Scher, H.I., Higgins, B., Rose, A., Cordon-Cardo, C., Thaler, H.T., Rifkind, R.A., Marks, P.A., and Richon, V.M. (2000). Suberoylanilide hydroxamic acid, an inhibitor of histone deacetylase, suppresses the growth of prostate cancer cells in vitro and in vivo. Cancer Res. *60*, 5165–5170.

Celis, J.E., and Celis, A. (1985). Cell cycle-dependent variations in the distribution of the nuclear protein cyclin proliferating cell nuclear antigen in cultured cells: subdivision of S phase. Proc. Natl. Acad. Sci. USA *82*, 3262–3266.

Chen, J.D., and Evans, R.M. (1995). A transcriptional co-repressor that interacts with nuclear hormone receptors. Nature *377*, 454–457.

Clarke, A.S., Lowell, J.E., Jacobson, S.J., and Pillus, L. (1999). Esa1p is an essential histone acetyltransferase required for cell cycle progression. Mol. Cell. Biol. *19*, 2515–2526.

Codina, A., Love, J.D., Li, Y., Lazar, M.A., Neuhaus, D., and Schwabe, J.W. (2005). Structural insights into the interaction and activation of histone deacetylase 3 by nuclear receptor corepressors. Proc. Natl. Acad. Sci. USA *102*, 6009–6014.

Ebert, B.L. (2009). Deletion 5q in myelodysplastic syndrome: a paradigm for the study of hemizygous deletions in cancer. Leukemia *23*, 1252–1256.

Gallinari, P., Di Marco, S., Jones, P., Pallaoro, M., and Steinkuhler, C. (2007). HDACs, histone deacetylation and gene transcription: from molecular biology to cancer therapeutics. Cell Res. *17*, 195–211.

Gilbert, N., and Allan, J. (2001). Distinctive higher-order chromatin structure at mammalian centromeres. Proc. Natl. Acad. Sci. USA *98*, 11949–11954.

Goodarzi, A.A., Noon, A.T., and Jeggo, P.A. (2009). The impact of heterochromatin on DSB repair. Biochem. Soc. Trans. *37*, 569–576.

Guenther, M.G., Barak, O., and Lazar, M.A. (2001). The SMRT and N-CoR corepressors are activating cofactors for histone deacetylase 3. Mol. Cell. Biol. *21*, 6091–6101.

Gunjan, A., and Verreault, A. (2003). A Rad53 kinase-dependent surveillance mechanism that regulates histone protein levels in *S. cerevisiae*. Cell *115*, 537–549.

Han, J., Zhou, H., Li, Z., Xu, R.M., and Zhang, Z. (2007). Acetylation of lysine 56 of histone H3 catalyzed by RTT109 and regulated by ASF1 is required for replisome integrity. J. Biol. Chem. *282*, 28587–28596.

Horlein, A.J., Naar, A.M., Heinzel, T., Torchia, J., Gloss, B., Kurokawa, R., Ryan, A., Kamei, Y., Soderstrom, M., Glass, C.K., et al. (1995). Ligand-independent repression by the thyroid hormone receptor mediated by a nuclear receptor co-repressor. Nature *377*, 397–404.

Iwabuchi, K., Basu, B.P., Kysela, B., Kurihara, T., Shibata, M., Guan, D., Cao, Y., Hamada, T., Imamura, K., Jeggo, P.A., et al. (2003). Potential role for 53BP1 in DNA end-joining repair through direct interaction with DNA. J. Biol. Chem. *278*, 36487–36495.

Johannsdottir, H.K., Jonsson, G., Johannesdottir, G., Agnarsson, B.A., Eerola, H., Arason, A., Heikkila, P., Egilsson, V., Olsson, H., Johannsson, O.T., et al. (2006). Chromosome 5 imbalance mapping in breast tumors from BRCA1 and BRCA2 mutation carriers and sporadic breast tumors. Int. J. Cancer *119*, 1052–1060.

Johnson, C.A., White, D.A., Lavender, J.S., O'Neill, L.P., and Turner, B.M. (2002). Human class I histone deacetylase complexes show enhanced catalytic activity in the presence of ATP and co-immunoprecipitate with the ATP-dependent chaperone protein Hsp70. J. Biol. Chem. *277*, 9590–9597.

Jones, P.L., and Shi, Y.B. (2003). N-CoR-HDAC corepressor complexes: roles in transcriptional regulation by nuclear hormone receptors. Curr. Top. Microbiol. Immunol. *274*, 237–268.

Karagianni, P., and Wong, J. (2007). HDAC3: taking the SMRT-N-CoRrect road to repression. Oncogene *26*, 5439–5449.

Knutson, S.K., Chyla, B.J., Amann, J.M., Bhaskara, S., Huppert, S.S., and Hiebert, S.W. (2008). Liver-specific deletion of histone deacetylase 3 disrupts metabolic transcriptional networks. EMBO J. *27*, 1017–1028.

Kondo, Y., Shen, L., Ahmed, S., Boumber, Y., Sekido, Y., Haddad, B.R., and Issa, J.P. (2008). Downregulation of histone H3 lysine 9 methyltransferase G9a induces centrosome disruption and chromosome instability in cancer cells. PLoS One *3*, e2037.

Lachner, M., O'Carroll, D., Rea, S., Mechtler, K., and Jenuwein, T. (2001). Methylation of histone H3 lysine 9 creates a binding site for HP1 proteins. Nature *410*, 116–120.

Li, W., Nagaraja, S., Delcuve, G.P., Hendzel, M.J., and Davie, J.R. (1993). Effects of histone acetylation, ubiquitination and variants on nucleosome stability. Biochem. J. *296*, 737–744.

Liao, Y.L., Sun, Y.M., Chau, G.Y., Chau, Y.P., Lai, T.C., Wang, J.L., Horng, J.T., Hsiao, M., and Tsou, A.P. (2008). Identification of SOX4 target genes using phylogenetic footprinting-based prediction from expression microarrays

suggests that overexpression of SOX4 potentiates metastasis in hepatocellular carcinoma. Oncogene *27*, 5578–5589.

Lieberman, H.B. (2008). DNA damage repair and response proteins as targets for cancer therapy. Curr. Med. Chem. *15*, 360–367.

Luger, K., and Richmond, T.J. (1998). The histone tails of the nucleosome. Curr. Opin. Genet. Dev. *8*, 140–146.

Luger, K., Mader, A.W., Richmond, R.K., Sargent, D.F., and Richmond, T.J. (1997). Crystal structure of the nucleosome core particle at 2.8 Å resolution. Nature *389*, 251–260.

Luijsterburg, M.S., Dinant, C., Lans, H., Stap, J., Wiernasz, E., Lagerwerf, S., Warmerdam, D.O., Lindh, M., Brink, M.C., Dobrucki, J.W., et al. (2009). Heterochromatin protein 1 is recruited to various types of DNA damage. J. Cell Biol. *185*, 577–586.

Madsen, P., and Celis, J.E. (1985). S-phase patterns of cyclin (PCNA) antigen staining resemble topographical patterns of DNA synthesis. A role for cyclin in DNA replication? FEBS Lett. *193*, 5–11.

Mahlknecht, U., Emiliani, S., Najfeld, V., Young, S., and Verdin, E. (1999). Genomic organization and chromosomal localization of the human histone deacetylase 3 gene. Genomics *56*, 197–202.

Marchion, D.C., Bicaku, E., Daud, A.I., Richon, V., Sullivan, D.M., and Munster, P.N. (2004). Sequence-specific potentiation of topoisomerase II inhibitors by the histone deacetylase inhibitor suberoylanilide hydroxamic acid. J. Cell. Biochem. *92*, 223–237.

Neumann, H., Hancock, S.M., Buning, R., Routh, A., Chapman, L., Somers, J., Owen-Hughes, T., van Noort, J., Rhodes, D., and Chin, J.W. (2009). A method for genetically installing site-specific acetylation in recombinant histones defines the effects of H3 K56 acetylation. Mol. Cell *36*, 153–163.

Olive, P.L., and Banath, J.P. (1995). Radiation-induced DNA double-strand breaks produced in histone-depleted tumor cell nuclei measured using the neutral comet assay. Radiat. Res. *142*, 144–152.

Pavesi, F., Lotzniker, M., Scarabelli, M., Garbagnoli, P., and Moratti, R. (1989). Efficiency of composite laboratory tests in the diagnosis of liver malignancies. Int. J. Biol. Markers *4*, 163–169.

Perissi, V., Aggarwal, A., Glass, C.K., Rose, D.W., and Rosenfeld, M.G. (2004). A corepressor/coactivator exchange complex required for transcriptional activation by nuclear receptors and other regulated transcription factors. Cell *116*, 511–526.

Peters, A.H., O'Carroll, D., Scherthan, H., Mechtler, K., Sauer, S., Schofer, C., Weipoltshammer, K., Pagani, M., Lachner, M., Kohlmaier, A., et al. (2001). Loss of the Suv39h histone methyltransferases impairs mammalian heterochromatin and genome stability. Cell *107*, 323–337.

Pijnappel, W.W., Schaft, D., Roguev, A., Shevchenko, A., Tekotte, H., Wilm, M., Rigaut, G., Seraphin, B., Aasland, R., and Stewart, A.F. (2001). The *S. cerevisiae* SET3 complex includes two histone deacetylases, Hos2 and Hst1, and is a meiotic-specific repressor of the sporulation gene program. Genes Dev. *15*, 2991–3004.

Qiu, L.W., Yao, D.F., Zong, L., Lu, Y.Y., Huang, H., Wu, W., and Wu, X.H. (2008). Abnormal expression of insulin-like growth factor-II and its dynamic quantitative analysis at different stages of hepatocellular carcinoma development. Hepatobiliary Pancreat. Dis. Int. *7*, 406–411.

Rokhlin, O.W., Scheinker, V.S., Taghiyev, A.F., Bumcrot, D., Glover, R.A., and Cohen, M.B. (2008). MicroRNA-34 mediates AR-dependent p53-induced apoptosis in prostate cancer. Cancer Biol. Ther. *7*, 1288–1296.

Schalch, T., Duda, S., Sargent, D.F., and Richmond, T.J. (2005). X-ray structure of a tetranucleosome and its implications for the chromatin fibre. Nature *436*, 138–141.

Siddik, Z.H. (2003). Cisplatin: mode of cytotoxic action and molecular basis of resistance. Oncogene *22*, 7265–7279.

Smith, E.R., Eisen, A., Gu, W., Sattah, M., Pannuti, A., Zhou, J., Cook, R.G., Lucchesi, J.C., and Allis, C.D. (1998). ESA1 is a histone acetyltransferase that is essential for growth in yeast. Proc. Natl. Acad. Sci. USA *95*, 3561–3565.

Sobel, R.E., Cook, R.G., Perry, C.A., Annunziato, A.T., and Allis, C.D. (1995). Conservation of deposition-related acetylation sites in newly synthesized histones H3 and H4. Proc. Natl. Acad. Sci. USA *92*, 1237–1241.

Spurling, C.C., Godman, C.A., Noonan, E.J., Rasmussen, T.P., Rosenberg, D.W., and Giardina, C. (2008). HDAC3 overexpression and colon cancer cell proliferation and differentiation. Mol. Carcinog. *47*, 137–147.

Su, C.H., Shann, Y.J., and Hsu, M.T. (2009). p53 chromatin epigenetic domain organization and p53 transcription. Mol. Cell. Biol. *29*, 93–103.

Sugimura, K., Fukushima, Y., Ishida, M., Ito, S., Nakamura, M., Mori, Y., and Okumura, K. (2010). Cell cycle-dependent accumulation of histone H3.3 and euchromatic histone modifications in pericentromeric heterochromatin in response to a decrease in DNA methylation levels. Exp. Cell Res. *316*, 2731–2746.

Sun, Y., Jiang, X., Xu, Y., Ayrapetov, M.K., Moreau, L.A., Whetstine, J.R., and Price, B.D. (2009). Histone H3 methylation links DNA damage detection to activation of the tumour suppressor Tip60. Nat. Cell Biol. *11*, 1376–1382.

Suzuki, M., Endo, M., Shinohara, F., Echigo, S., and Rikiishi, H. (2009). Enhancement of cisplatin cytotoxicity by SAHA involves endoplasmic reticulum stress-mediated apoptosis in oral squamous cell carcinoma cells. Cancer Chemother. Pharmacol. *64*, 1115–1122.

Swift, L.P., Rephaeli, A., Nudelman, A., Phillips, D.R., and Cutts, S.M. (2006). Doxorubicin-DNA adducts induce a non-topoisomerase II-mediated form of cell death. Cancer Res. *66*, 4863–4871.

Taddei, A., Roche, D., Sibarita, J.B., Turner, B.M., and Almouzni, G. (1999). Duplication and maintenance of heterochromatin domains. J. Cell Biol. *147*, 1153–1166.

Tsukamoto, Y., Kato, J., and Ikeda, H. (1997). Silencing factors participate in DNA repair and recombination in *Saccharomyces cerevisiae*. Nature *388*, 900–903.

Verreault, A., Kaufman, P.D., Kobayashi, R., and Stillman, B. (1996). Nucleosome assembly by a complex of CAF-1 and acetylated histones H3/H4. Cell *87*, 95–104.

Wilson, A.J., Byun, D.S., Popova, N., Murray, L.B., L'Italien, K., Sowa, Y., Arango, D., Velcich, A., Augenlicht, L.H., and Mariadason, J.M. (2006). Histone deacetylase 3 (HDAC3) and other class I HDACs regulate colon cell maturation and p21 expression and are deregulated in human colon cancer. J. Biol. Chem. *281*, 13548–13558.

Wurmbach, E., Chen, Y.B., Khitrov, G., Zhang, W., Roayaie, S., Schwartz, M., Fiel, I., Thung, S., Mazzaferro, V., Bruix, J., et al. (2007). Genome-wide molecular profiles of HCV-induced dysplasia and hepatocellular carcinoma. Hepatology *45*, 938–947.

Xu, X.R., Huang, J., Xu, Z.G., Qian, B.Z., Zhu, Z.D., Yan, Q., Cai, T., Zhang, X., Xiao, H.S., Qu, J., et al. (2001). Insight into hepatocellular carcinogenesis at transcriptome level by comparing gene expression profiles of hepatocellular carcinoma with those of corresponding noncancerous liver. Proc. Natl. Acad. Sci. USA *98*, 15089–15094.

Yu, J., Palmer, C., Alenghat, T., Li, Y., Kao, G., and Lazar, M.A. (2006). The corepressor silencing mediator for retinoid and thyroid hormone receptor facilitates cellular recovery from DNA double-strand breaks. Cancer Res. *66*, 9316–9322.

Yuan, J., Pu, M., Zhang, Z., and Lou, Z. (2009). Histone H3-K56 acetylation is important for genomic stability in mammals. Cell Cycle *8*, 1747–1753.

Zhou, J., Zhou, B.O., Lenzmeier, B.A., and Zhou, J.Q. (2009). Histone deacetylase Rpd3 antagonizes Sir2-dependent silent chromatin propagation. Nucleic Acids Res. *37*, 3699–3713.

Zhuang, J., Jiang, G., Willers, H., and Xia, F. (2009). Exonuclease function of human Mre11 promotes deletional nonhomologous end joining. J. Biol. Chem. *284*, 30565–30573.